Efficient generation of correlated photon pairs in a microstructure fiber

J. Fan and A. Migdall

Optical Technology Division, National Institute of Standards and Technology, 100 Bureau Drive, Mail Stop 8441, Gaithersburg, Maryland 20899-8441

L. J. Wang

Max-Planck Research Group for Optics, Information and Photonics, and University of Erlangen, G.-Scharowsky Strasse 1, 91058 Erlangen, Germany

Received June 17, 2005; revised manuscript received August 8, 2005; accepted August 8, 2005

We report efficient generation of correlated photon pairs through degenerate four-wave mixing in a microstructure fiber. With 735.7 nm pump pulses producing correlated signal (688.5 nm) and idler (789.8 nm) photons in a 1.8 m microstructure fiber, we detect photon pairs at a rate of 37.6 kHz with a coincidence/accidental contrast of 10:1 with $\Delta\lambda = 0.7$ nm. This is the highest rate to our knowledge reported to date in a fiber-based photon source. The light source is highly nonclassical as defined by the Zou–Wang–Mandel inequality, which is violated by 1100 times the uncertainty.

OCIS codes: 190.4380, 270.5290.

Quantum information science based on the quantum entanglement between multiple parties is fundamentally changing the way we view information and our physical world. Research in these areas has made rapid progress in recent years, although many daunting tasks remain.[1–4] In particular, the practical success of many quantum communication and cryptography applications will require a robust source of correlated photon pairs.

Microstructure fiber (MF), with its central silica core surrounded by patterned air holes, can have very small effective mode diameters (1 to 2 μm), allowing for high field intensities and a wide range of wavelengths (400–1500 nm) that can propagate as a single spatial mode.[5] These effects greatly increase optical nonlinearities in the fiber and facilitate photon collection. Four-wave mixing (FWM) in MF is starting to be considered a correlated photon source[6–9] alternative to the well-accepted method relying on parametric downconversion (PDC).[10–14]

Degenerate FWM and reversed degenerate FWM schemes have been demonstrated in MF to generate correlated photon pairs.[6–9] By injecting a single optical pump wavelength into MF in the negative or zero dispersion spectral regions of the fiber, two photons (ω_p) from the pump field are absorbed to create a pair of signal (ω_s) and idler photons (ω_i) under the FWM condition $\omega_s + \omega_i = 2\omega_p$. Contrasts between coincidence and accidental coincidence rates (C/A) of 2:1 have been demonstrated.[6,7] Moving the optical pump to the normal dispersion spectral region of the fiber has improved the C/A contrast to 5:1.[8] Recently we demonstrated a conjugate pump scheme that is a reversed degenerate FWM process. A pair of pump beams at conjugate frequencies, with respect to the zero dispersion frequency of the fiber, serve as the input. One photon from each of the two pump beams is absorbed to create a correlated photon pair at the middle frequency under the FWM condition.[9] In that experiment, the highest C/A contrast measured was 8:1.

For high-speed and high-fidelity quantum communication and cryptography applications, two basic conditions are required for the correlated photon source—a high coincidence rate and a high C/A contrast. Here, we report significant advances in each of these parameters achieved by using a fiber-based correlated photon source and a degenerate FWM scheme. With signal and idler photons separated in wavelength by 100 nm, we achieve a coincidence rate of 37.6 kHz with a C/A contrast of 10:1 with a collection bandwidth $\Delta\lambda = 0.7$ nm in free-space operation. This is the highest measured rate per bandwidth in a fiber-based photon source to date to our knowledge.

As shown in Fig. 1, we couple linearly polarized laser pulses from a Ti:sapphire oscillator into a 1.8 m MF, with polarization along one of the principal axes of the MF. The laser wavelength is 735.7 nm (with $\Delta\lambda = 0.1$ nm), which is the zero dispersion wavelength of the MF. The broadband output from the MF is directed to a high-efficiency grating (1800 lines/mm). A two-pass grating geometry is used to spectrally spread, select, and then reimage the beam to achieve efficient single-mode collection. The selected signal and idler wavelengths are $\lambda_s = 688.5$ nm and $\lambda_i = 789.8$ nm, each with $\Delta\lambda = 0.7$ nm set by an adjustable slit. Interference filters ($\Delta\lambda = 10$ nm) at the collection lenses suppress scattered pump and stray light. The signal and idler photons are coupled into single-mode fibers and detected by photon counters and a coincidence circuit,[9] with overall detection efficiencies experimentally determined to be $\eta_s = 0.097$ for signal photons and $\eta_i = 0.076$ for idler photons. In this experiment, photon generation rates in the signal and the idler bandwidths are kept below 0.1 photons per pulse.

In MF, the phase-matching condition for FWM is $(2k_p - k_s - k_i) - 2\gamma P/(R\tau) = 0$,[15] where k_p, k_s, and k_i are

0146-9592/05/243368-3/$15.00

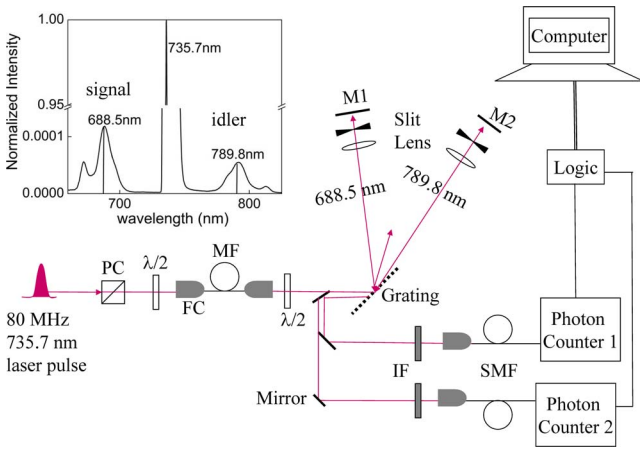

Fig. 1. (Color online) Schematic experimental setup. PC, polarizer; FC, fiber coupler; SMF; single mode fiber; λ/2, half-wave plate; IF, interference filters; M1, M2 mirrors; MF, microstructure fiber. The inset is a normalized spectrum of the output from the MF at an average pump power of 12 mW.

longitudinal wavenumbers for the pump, signal, and idler photons in the fiber, $\gamma=110/\mathrm{km/W}$ is the nonlinearity coefficient of the fiber, P is the average pump power, $\tau=8$ ps is the pump pulse width, and $R=80$ MHz is the laser repetition rate. With $P=0.5$ mW the detected C/A contrast strongly peaks at $\lambda_s=688.5$ nm when we scan the wavelength of the signal beam [Fig. 2(a)], giving $\Delta\lambda=0.9$ nm. This peak, resulting from the phase-matching condition, is the signature of FWM in a MF.

For fixed pump and idler wavelengths, a variation of pump power $\delta P=1$ mW produces a negligible variation of the phase-matched signal wavelength compared with our collection bandwidths, so the power-dependent measurement of photon coincidence can be carried out without changing the collection wavelengths.

Figure 2(b) shows the signal and idler count rates as a function of P, both exhibiting strong quadratic dependence with pump power. Because Raman scattering is the main noise source competing with the two-photon process in fiber,[16] and it is biased toward longer wavelengths,[15] the idler rate exceeds the signal rate even though $\eta_s > \eta_i$. A maximum coincidence rate of 37.6 kHz with a C/A contrast of 10:1 with $\Delta\lambda=0.7$ nm at $P=1$ mW is shown in Figs. 2(c) and 2(d). This exceeds the recent record rate of 6.8 kHz with $\Delta\lambda=5$ nm to 10 nm at $P=100$ mW.[8]

We attribute this high coincidence and high contrast to several advantages of our scheme. First, it is known that the gains of FWM and spontaneous Raman scattering are not uniform with wavelength, so it is possible to optimize the FWM relative to the Raman signals. In our experiment, this requires placing the signal and idler wavelengths in the first-order FWM gain spectral regions shown in the inset of Fig. 1. This wavelength arrangement enables us to achieve a high photon pair production rate with a relatively low noise level in the MF. This optimization method relies on the spectral selectivity of the phase-matching feature of FWM, the Raman gain profile, and dispersion property of the silica fiber. We expect to achieve a similar advantage in any silica-based high-nonlinearity MF with similar Raman response and dispersion property. A second advantage is the high nonlinearity ($\gamma=110/\mathrm{km/W}$), which results from the small effective mode diameter (1.2 μm) of the MF, and the associated increased intensity. Last, we retain single-mode collection with the two-pass grating arrangement (this could just as well be replaced by an all-fiber wavelength demultiplexer for high efficiency and multichannel operation). These three advantages together make possible our MF-based photon source's high correlated pair detection rate and high C/A contrast relative to other previous experiments.[6–9]

For rate per milliwatt pump power and per nanometer collection spectral bandwidth, the present result (53.7 kHz/mW/nm) also exceeds coincidence rates by a PDC in bulk crystals (0.2 kHz/mW/nm)[14] and is comparable with the rates achieved by PDC in poled crystal waveguide sources (~50 kHz/mW/nm).[17–19] A high C/A contrast of 300:1 is obtained at 50 μW with a coincidence rate of 45 Hz.

The contribution of FWM to photon generation in the MF can be characterized by the ratios of the photon pair generation rate to the signal or idler photon generation rates, defined by $r_s=(D_c-D_a)/(\eta_i D_s)$ and $r_i=(D_c-D_a)/(\eta_s D_i)$, where D_c and D_a are measured coincidence and accidental rates and D_s and D_i are measured signal and idler rates. In our experiment we find $r_s=96\%$ and $r_i=50\%$ at $P=1$ mW and $r_s=58\%$ and $r_i=4\%$ at 50 μW, showing that FWM dominates photon generation at λ_s, while Raman scattering dominates photon generation at λ_i, especially at the lower power.

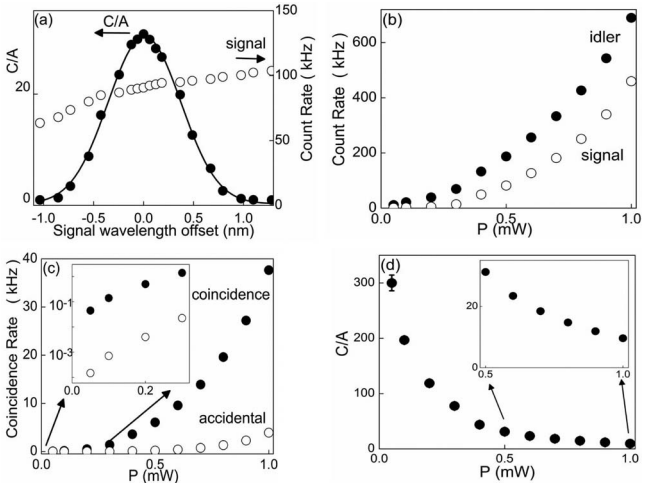

Fig. 2. (a) Spectral scan of C/A (filled dots) and signal photon count rate (open dots) as the signal channel is tuned around the central phase-matching wavelength $\lambda_s=688.5$ nm (corresponding to a zero wavelength offset) with $\lambda_{\mathrm{pump}}=735.7$ nm and $\lambda_i=789.8$ nm, with $P=0.5$ mW. C/A is fit to a Gaussian function (solid curve). (b) Signal (opened dots) and idler photon count rates (filled dots). (c) Detected coincidence rate (filled dots) and accidental coincidence rate (open dots). (d) Contrast between the measured coincidence and accidentals. For (a) to (d), each data point is averaged over 30 s for $P \geq 0.4$ mW and 600 s for $P < 0.4$ mW.

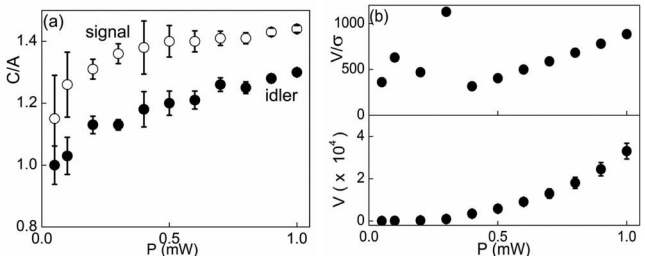

Fig. 3. (a) Self-correlation measurements for signal (open dots) and idler photons (filled dots) as a function of the pump power. (b) V (lower) and V/σ (upper) versus P, with V error bars expanded by 100× for a better view. For (a) and (b), each data point is averaged over 30 s for $P \geq 0.4$ mW and 600 s for $P < 0.4$ mW.

The high coincidence rates observed can be explained only qualitatively with the simple FWM theory developed for a cw optical pump by using the slowly varying amplitude approximation.[20] The theory predicts a coincidence rate of $\eta|\gamma P z|^2 \Delta\nu/(\pi R) \approx 160$ kHz at $P=1$ mW, which is within an order of magnitude of the measured coincidence rate. Here z is the fiber length, $\Delta\nu$ is the detection bandwidth, and $\eta=0.0074$ is the detection efficiency for a photon pair. To further examine the photon generation process, we split signal (or idler) photons into two equal beams and examine photon coincidences between them. Self-correlations characterized by the contrast C/A exceed 1 for both signal and idler photons as shown in Fig. 3(a). This shows that multiphoton processes such as the stimulated Raman process are involved in photon generation in the MF, which could increase the photon coincidence rate, but not to a significant level, as indicated by the low contrast for self-correlation. To quantify photon generation in a MF, the nonlinear propagation process of picosecond laser pulses in a MF is being studied.

If the MF is a nonclassical photon source, the coincidence count rate resulting from the cross correlation between signal and idler photons should be greater than twice the sum of the self-correlated coincidence rates of signal photons and idler photons.[21] Defining $V=(D_c-D_a)-2(D_s-D_{s,a}+D_i-D_{i,a})$, where D_c and D_a are the detected cross-correlated coincidence and accidental rates and $D_s(D_i)$ and $D_{s,a}(D_{i,a})$ are the detected self-correlated coincidence and accidentals. For a nonclassical source, we have the Zou–Wang–Mandel inequality $V>0$. V is measured and plotted in Fig. 3(b). The error bars represent 1σ, the combined standard uncertainty. The nonclassicality violation characterized by the ratio of V/σ ranges from 360 to 1100.

In conclusion, we have experimentally demonstrated the generation of correlated photons in an MF. In a simple system, we have obtained a high twin photon coincidence rate of 53.7 kHz/mW/nm with a contrast of 10:1. To our knowledge this is the highest detection rate of correlated photon pairs in a single-mode fiber-based photon source scheme. The highly nonclassical light source violates a classical inequality by up to 1100σ. We also show that a coincidence/accidental contrast as high as 300:1 can be achieved, albeit at lower count rates. These high contrasts may be particularly useful in some fundamental tests of quantum mechanics. Our experiment suggests that a practical polarization-entangled correlated photon source[22] can be realized by using MF, and that possibility is being pursued.

This work has been supported by the Multidisciplinary University Research Initiative Center for Photonic Quantum Information Systems (Army Research Office/Advanced Research and Development Activity program DAAD19-03-1-0199) and the Defense Advanced Research Projects Agency/Quist program. L. J. Wang acknowledges the support by Japan Science and Technology Foundation (JST) under the Core Research for Evolutional Science and Technology (CREST) program. J. Fan's email address is Jfan@nist.gov.

References

1. D. Bouwmeester, J. W. Pan, K. Mattle, M. Eibl, H. Weinfurter, and A. Zeilinger, Nature **390**, 575 (1997).
2. A. Furusawa, J. Sorensen, S. L. Braunstein, C. Fuchs, H. J. Kimble, and E. S. Polzik, Science **282**, 706 (1998).
3. C. Kurtsiefer, P. Aarda, M. Halder, H. Weinfurter, P. M. Gorman, and P. R. Tapster, Nature **419**, 450 (2002).
4. M. Aspelmeyer, H. R. Böhm, T. Gyatso, T. Jennewein, R. Kaltenbaek, M. Lindenthal, G. Molina-Terriza, A. Poppe, K. Resch, M. Taraba, R. Ursin, P. Walther, and A. Zeilinger, Science **301**, 621 (2003).
5. J. C. Knight, T. A. Birks, P. St. J. Russell, and D. M. Atkin, Opt. Lett. **21**, 1547 (1996).
6. A. Dogariu, J. Fan, and L. J. Wang, NEC Res. Dev. **44**, 294 (2003).
7. J. E. Sharping, J. Chen, X. Li, and P. Kumar, Opt. Express **12**, 3086 (2004).
8. J. G. Rarity, J. Fulconis, J. Duligall, W. J. Wadsworth, and P. St. J. Russell, Opt. Express **13**, 534 (2005).
9. J. Fan, A. Dogariu, and L. J. Wang, Opt. Lett. **30**, 1530 (2005).
10. D. C. Burnham and D. L. Weinberg, Phys. Rev. Lett. **25**, 84 (1970).
11. S. Friberg, C. K. Hong, and L. Mandel, Phys. Rev. Lett. **54**, 2011 (1985).
12. S. Friberg, C. K. Hong, and L. Mandel, Opt. Commun. **54**, 311 (1984).
13. P. G. Kwiat, E. Waks, A. G. White, I. Appelbaum, and P. H. Eberhard, Phys. Rev. A **60**, 773(R) (1999).
14. C. Kurtsiefer, M. Oberparleiter, and H. Weinfurter, Phys. Rev. A **64**, 023802 (2001).
15. G. P. Agrawal, *Nonlinear Fiber Optics* (Academic, 1995).
16. X. Li, J. Chen, P. Voss, J. E. Sharping, and P. Kumar, Opt. Express **12**, 3737 (2004).
17. S. Tanzilli, W. Tittel, H. D. Riedmatten, H. Zbinden, P. Baldi, M. DeMicheli, D. B. Ostrowsky, and N. Gisin, Eur. Phys. J. D **18**, 155 (2002).
18. A. B. U'Ren, C. Silberhorn, K. Banaszek, and I. A. Walmsley, Phys. Rev. Lett. **93**, 093601 (2004).
19. F. Konig, E. J. Mason, F. N. C. Wong, and M. A. Albota, Phys. Rev. A **71**, 03380 (2005).
20. L. J. Wang, C. K. Hong, and S. R. Friberg, J. Opt. Soc. Am. B **3**, 346 (2001).
21. X. Y. Zou, L. J. Wang, and L. Mandel, Opt. Commun. **84**, 351 (1991).
22. X. Li, P. Voss, J. E. Sharping, J. Chen, and P. Kumar, Phys. Rev. Lett. **94**, 053601 (2005).